A&A 503, 883–888 (2009)
DOI: 10.1051/0004-6361/200810909

Astronomy & Astrophysics

Plausible explanations for the variations of orbital period in the old nova DQ Herculis*

Z. B. Dai[1,2,3] and S. B. Qian[1,2]

[1] National Astronomical Observatories/Yunnan Observatory, Chinese Academy of Sciences, PO Box 110, 650011 Kunming, PR China
e-mail: zhibin_dai@ynao.ac.cn
[2] United Laboratory of Optical Astronomy, Chinese Academy of Science (ULOAC), 100012 Beijing, PR China
[3] Graduate School of the CAS, Beijing, PR China

Received 4 September 2008 / Accepted 28 April 2009

ABSTRACT

Aims. Several mechanisms are presented to explain the observed small variation in the orbital period of the old nova DQ Herculis.
Methods. We have combined two new CCD times of light minimum of DQ Herculis with all 226 available times of light minimum, including 79 visual observations, for the new orbital period analysis.
Results. Based on this analysis, the best-fit of the O–C diagram for DQ Herculis is a quadratic-plus-sinusoidal fit. A secular orbital period increase with a rate of $9.5(\pm0.1) \times 10^{-12}$ s s^{-1} is confirmed, which corresponds to a lower limit of the mass transfer rate of $7.2(\pm3.2)\times10^{-9}$ $M_\odot$ yr^{-1}. We investigate three plausible mechanisms (direct change of the red dwarf's radius, Applegate's mechanism and the light travel-time effect) to explain the quasi-periodic variation shown in the O–C diagram. Although previous works have suggested that solar-type magnetic cycles in the red dwarf can explain the quasi-periodic variation in the orbital period, we were not able to reproduce this finding. Accordingly, a light trave-time effect is proposed, with a brown dwarf as a tertiary component with a significance level of $\gtrsim$77.8% orbiting around nova DQ Herculis. In order to interpret the small departure from the best-fit near 60 000 cycles, we assume an eccentric orbit of the third body with a small eccentricity. However, a satisfying result was obtained because the eccentricity $e = 0.12$ is close to zero. The parameters of this elliptical orbit are similar to that of a circular orbit.

Key words. stars: novae, cataclysmic variables – stars: binaries: eclipsing – stars: individual: DQ Herculis

1. Introduction

The remnant of the nova Herculis 1934, named DQ Herculis, was first detected at a magnitude of $3^{\mathrm{m}}.3$ (Campbell 1935). It is not only a well-observed prototype of intermediate Polar stars, but also a moderately slow galactic nova. This means that the binary system not only contains a white dwarf with a strong magnetic field, which can partially control the accreting stream from the red dwarf along the magnetic field lines to fall onto one or both magnetic poles of the white dwarf (Patterson 1994), but also has thermonuclear runaway on the surface of the white dwarf (Starrfield 1989). The discovery of eclipses in DQ Herculis (Walker 1956) was pivotal in establishing the standard picture of cataclysmic variables. At the same time, Walker (1956) reported a coherent 71 s photometric oscillation. The spectral type of the red dwarf is estimated to be M3 due to the detection of faint TiO bands (Young & Schneider 1981). Since DQ Herculis is an eclipsing binary with an orbital period of $4^{\mathrm{h}}39^{\mathrm{m}}$ and has been extensively observed, its properties are well known. For example, recent estimations of $M_1 = 0.6$ $M_\odot$ and $M_2 = 0.4$ $M_\odot$ (Horne et al. 1993) correct the previous results from earlier works (e.g. Robinson 1976; Smak 1980).

Since the mass transfer in DQ Herculis detected by Kraft (1959), a variation in the orbital period is expected. Mumford (1969) and Nather & Warner (1969) suggested that the orbital period is increasing, and later works (Patterson et al. 1978; Africano & Olson 1981; Zhang et al. 1995; Wood et al. 2005) indicated that a sinusoidal modulation with a period of ∼14 yr is likely. However, an updated O–C analysis (Wood et al. 2005) concluded that there is not strong evidence for a secular orbital period increase. They did not produce an explanation for the cyclical variation in the O–C diagram of DQ Herculis. According to Patterson et al. (1978), light travel-time effects cannot be applied to explain the O–C cyclic variation because a similar variation is not present in the 71 s oscillation timings. Therefore, there is no convincing explanation for the orbital period variation of DQ Herculis so far.

226 available times of light minimum from 1954 to 2008 are presented in Sect. 2, including two new data points from our observations and 79 visual data points. Section 3 gives the O–C analysis for DQ Herculis. A discussion of the possible mechanisms for orbital period change is given in Sect. 4.

2. Observation of times of light minimum

Two new times of light minimum are obtained from our CCD photometric observations with the PI1024 TKB CCD photometric system attached to the 1.0-m reflecting telescope at the Yunnan Observatory in China. The first CCD photometric observation of DQ Herculis was carried out on February 10, 2008 in white light, and the second observation on March 28, 2008 was through the R-filter, which is close to the Johnson standard photometric system. Two nearby stars that have a similar brightness in the same viewing field of the telescope were chosen as the comparison star and the check star. All images were reduced by using PHOT (measured magnitudes for a list of stars) in the aperture photometry package of IRAF. Two CCD times of light

* Table 1 is only available in electronic form at http://www.aanda.org

Article published by EDP Sciences

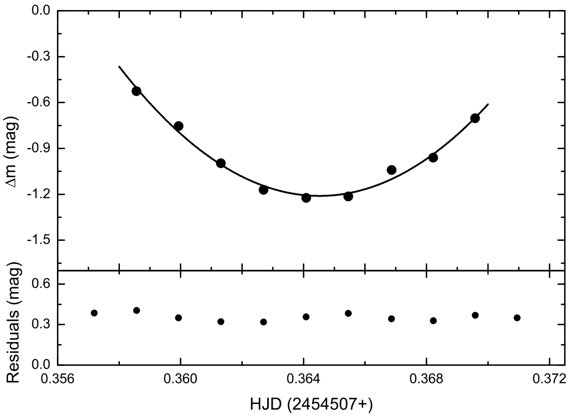

Fig. 1. The light curve of the eclipsing part of DQ Herculis shown in the upper figure, obtained on Feb. 10, 2008 in white light. The solid line represents the best parabolic fit. The lower figure shows the residuals of differential photometry.

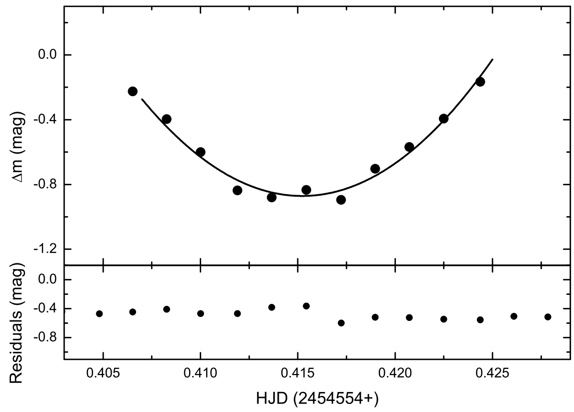

Fig. 2. Upper panel is the *R*-band light curve of the eclipsing part of DQ Herculis obtained on Mar. 28, 2008. The solid line represents the best parabolic fit. The lower figure shows the residuals of differential photometry.

minimum were derived by using a parabolic fitting method. Both light curves of eclipsing parts and their parabolic fits are displayed in upper planes of Figs. 1 and 2, respectively. The residuals of differential photometries shown in the lower planes of Figs. 1 and 2 suggest that the times of light minimum in our observations can be derived by a parabolic fit with high precision.

As the two new eclipsing times obtained from CCD observations are to 4 significant figures, we infer that the previous times of light minimum obtained by using photographic or visual methods without given error, should have lower accuracy. Therefore, we assume that the CCD or photoelectric data and the photographic or visual data without given errors have default errors of $0\overset{\mathrm{d}}{.}0001$ and $0\overset{\mathrm{d}}{.}001$, respectively. The collected times of light minimum were checked again because some data were obtained from many years ago, and some identical times of light minimum may have small differences, as they were observed at different observatories or in different filters. In this case, the average value should be reliable and may be applied. In addition, Zhang et al. (1995) and Wood et al. (2005) reported their 44 eclipse times in Heliocentric Julian Ephemeris Dates (HJED), which correspond to ephemeris time (ET). Thus, we converted them to Heliocentric Julian Dates (HJD), which correspond to coordinated Universal time (UTC). All 226 available times of light minimum covering half a century listed in Table 1 have been checked carefully, and those obviously inaccurate were corrected or abandoned. For example, the 7 photographic data points before 1954 are not used in this paper because of the very large scatter.

3. Analysis of orbital period changes

The ephemeris derived by Africano & Olson (1981) is used to calculate the O–C values of DQ Herculis and, after linear revision, the new epochs and average orbital period of DQ Herculis were derived as

$$T_{\min} = \mathrm{HJD}\ 2\,434\,954.94306(2) + 0\overset{\mathrm{d}}{.}1936209219(3)E, \quad (1)$$

with variance $\sigma_1 = 1\overset{\mathrm{d}}{.}42 \times 10^{-3}$. The O–C values versus epoch numbers are plotted in Fig. 3 which suggests a trend of cyclic variation. Although Wood et al. (2005) pointed out that a sinusoidal fit is formally significant but not compelling, the two new eclipsing times we obtained could alter this conclusion because the O–C values since 1985 cannot be fitted by a straight line. Moreover, we suggested that the most important cause of the

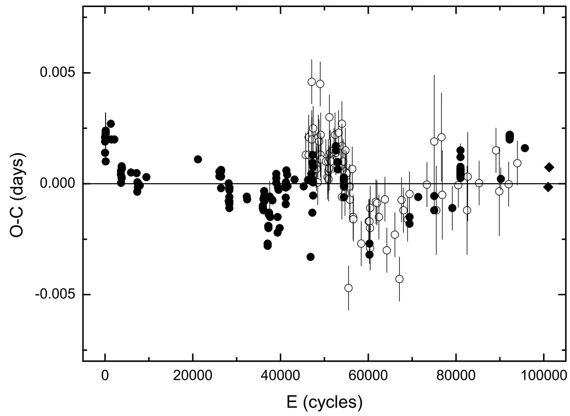

Fig. 3. The O–C values calculated with Eq. (1) versus the cycles. The 79 visual data points and the photoelectric or CCD data are plotted as open circles and solid circles, respectively.

non-compelling sine fit is the neglect of a quadric term in the O–C analysis. Accordingly, based on all 226 data points, a least-square solution of the quadric ephemeris leads to

$$\begin{aligned}(\mathrm{O-C})_1 &= 0\overset{\mathrm{d}}{.}00112(\pm 0\overset{\mathrm{d}}{.}00002) - 7\overset{\mathrm{d}}{.}6(\pm 0\overset{\mathrm{d}}{.}1) \times 10^{-8}E \\ &\quad + 8\overset{\mathrm{d}}{.}4(\pm 0\overset{\mathrm{d}}{.}1) \times 10^{-13}E^2, \end{aligned} \quad (2)$$

with variance $\sigma_{2q} = 1\overset{\mathrm{d}}{.}38 \times 10^{-3}$. This quadric fit and its residuals (i.e. $(\mathrm{O-C})_2$) are presented in the top and middle planes of Fig. 4, respectively. The O–C diagram, after removing the quadric term shown in middle planes of Fig. 4, also shows a cyclical period change. A simple sinusoidal function is used to fit the $(\mathrm{O-C})_2$ and a least-square solution yields

$$\begin{aligned}(\mathrm{O-C})_2 &= 3\overset{\mathrm{d}}{.}1(\pm 0\overset{\mathrm{d}}{.}1) \times 10^{-4} \sin[0.011^\circ(\pm 0.0002^\circ)E \\ &\quad + 90.0^\circ(\pm 3.4^\circ)], \end{aligned} \quad (3)$$

with variance $\sigma_{2s} = 1\overset{\mathrm{d}}{.}25 \times 10^{-3}$. Using the statistic parameter λ of the F-test as defined by Pringle (1975), we obtained $F(1, 223) = 13.1$, which corresponds to $a > 99.99\%$ confidence level for the existence of quadric term. However, since the simple sine fit fails the F-test, we performed a regular χ^2-test to measure the goodness-of-fit of Eq. (3). The calculated parameter $\chi^2 = 39.9$ indicates that it is a significant fit. Since the simple fit cannot simultaneously adjust the quadric term and the sinusoidal term in the O–C diagram to search for a best fit, in order to further reduce the residuals we attempted to use a simultaneous quadratic-plus-sinusoidal formula to fit this variation. The

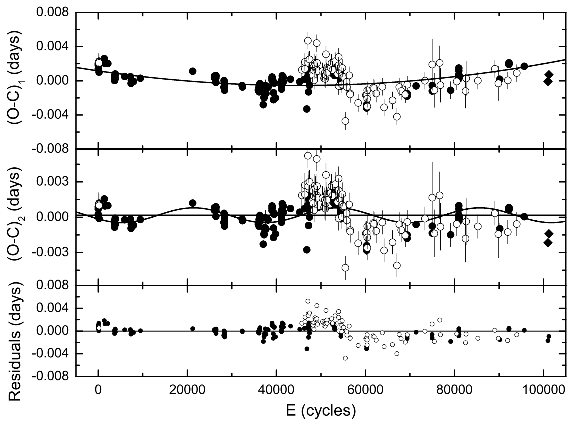

Fig. 4. The O–C values of DQ Herculis fitted with the formulas displayed in Eqs. (2) and (3). The fitting curves are plotted in the top and middle figure, respectively. The residuals and their linear fitted solid line are presented in the bottom plane.

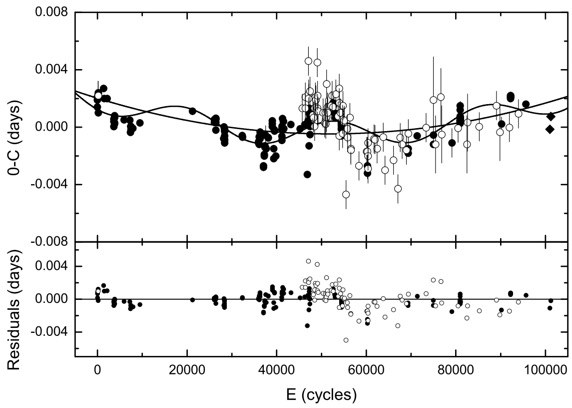

Fig. 5. The O–C values of DQ Herculis obtained from the elements in Eq. (4). The fitting curves are plotted in the top figure. The residuals are presented in the bottom plane.

least-square solution leads to

$$\begin{aligned} \text{O–C} \;=\; & 2^{\rm d}\!.01(\pm 0^{\rm d}\!.03)\times 10^{-3} - 9^{\rm d}\!.6(\pm 0^{\rm d}\!.1)\times 10^{-8}E \\ & +9^{\rm d}\!.2(\pm 0^{\rm d}\!.1)\times 10^{-13}E^2 + 8^{\rm d}\!.9(\pm 0^{\rm d}\!.2)\times 10^{-4} \\ & \times \sin[0.0108^\circ(\pm 0.0002^\circ)E + 60.9^\circ(\pm 0.9^\circ)] \end{aligned} \qquad (4)$$

with variance $\sigma_3 = 1^{\rm d}\!.17\times 10^{-3}$. The residuals are displayed in the bottom panel of Fig. 5. The F-test to assess the significance of the quadratic and sinusoidal terms in Eq. (4) is valid, as long as the parameter λ is corrected to be

$$\lambda = \frac{(\sigma_1^2 - \sigma_3^2)/4}{\sigma_3^2/(n-6)}, \qquad (5)$$

where n is the number of data points. Thus, a calculation gives $F(4, 220) = 26.0$, which indicates that it is significant well above the 99.99% level. Therefore, both separate and simultaneous fits suggest that the best-fit of the O–C diagram for DQ Herculis should be the ~17.7(±0.3) yr quasi-periodic modulation shown in the top and middle panels of Fig. 5 superimposed on a secular orbital period increase. The variational period ~17.7(±0.3) yr is in agreement with the result of ~14 yr from earlier works. The sine curve shown in the top panel of Fig. 5 does not well describe the visual data of 60 000 cycles observed in 1985, as is also shown in Wood et al. (2005). Although this poor fit is caused mainly by the visual data, two photoelectric observations at cycles 60 281 and 60 286, also present a large departure from the fit, as the visual data do. This means that the visual data may show a real episode of variation of the eclipse minima. Therefore, the variation in the O–C diagram should be quasi-periodic, as discussed in Sect. 4.

Although Pringle (1975), Africano & Olson (1981) and Wood et al. (2005) suggested that the orbital period of DQ Herculis is constant, the residuals of this quadratic-plus-sinusoidal fit shown in the bottom panel of Fig. 5 never show a detectable variation, which implies the existence of quadratic variation in O–C diagram. Moreover, the standard model of cataclysmic variables (Warner & Nather 1971; Smak 1971) indicates that mass transfer is a common phenomena. According to the coefficient of the quadratic term in Eq. (4), the orbital period change rate of DQ Herculis, $\dot{P}$, can be calculated to be $9.5(\pm 0.1)\times 10^{-12}$ s s^{-1}.

4. Discussion

4.1. Secular orbital period increase

Considering that the secular orbital period change for DQ Herculis remains a matter of debate, the mass transfer between both components may be low or non-existent, a situation that corresponds to the presence of a faint hot spot in many eclipse light curves of DQ Herculis (Bianchini et al. 2004). Although the accurate masses of both components are still not available, it is definite that the mass ratio, $q = M_2/M_1$, is less than unity. Therefore, mass transfer from the red dwarf to the white dwarf is a very reasonable explanation for the orbital period increase shown in Figs. 4 and 5. According to Kepler's third law, the orbital period change with conservation can be given by

$$\frac{\dot{P}}{P} = 3\frac{M_2 - M_1}{M_1}\frac{\dot{M}_2}{M_2}, \qquad (6)$$

where $\dot{M}_2$ is mass transfer rate from the red dwarf. Using the masses of both components ($M_1 = 0.6(\pm 0.07)\ M_\odot$ and $M_2 = 0.4(\pm 0.05)\ M_\odot$) derived by Horne et al. (1993), a lower limit of the mass transfer rate, $\dot{M}_2 = -7.2(\pm 3.2)\times 10^{-9}\ M_\odot\ {\rm yr}^{-1}$ is obtained, which is the same order of magnitude as that derived by Zhang et al. (1995), and should be considered as a lower limit. Thus, if there are extra mechanisms of mass and angular momentum loss in DQ Herculis, then a considerable mass transfer rate from the red dwarf to the white dwarf is needed to produce the observed orbital period increase.

4.2. Quasi-periodic variation

4.2.1. Variations of the red dwarf's radius

A ~17.7(±0.3) *yr* quasi-period variations is seen in the O–C diagram of DQ Herculis. Warner (1988) applied a technique sensitive to mass overflow, which means that the mass transfer from the red dwarf can be changed by a slight variation of its radius. This can explain the cyclical change in the O–C diagram. He proposed that a change in radius of the tidally distorted secondary star is the result of solar-type magnetic cycles. The variation of radius of the red dwarf, ΔR, can be described as,

$$\frac{\Delta R}{R} = A\sin(\Omega\, t), \qquad (7)$$

where A is the amplitude of radius variations. The modulation of mass transfer rate $\dot{M}$ caused by radius variation is given by

$$\dot{M} = \dot{M}_0\ {\rm e}^{3.1\times 10^3 \frac{\Delta R}{R}}, \qquad (8)$$

where $\dot{M}_0$ is the rate for the undisturbed state (i.e. $\Delta R = 0$) and the times of eclipse minima will vary as (Warner 1988)

$$\text{(O–C)}_{\text{orbital}} = 13.0 k_2 q^{2/3}(1+q)^{-5/3}\frac{A}{\Omega}\cos(\Omega\, t), \quad (9)$$

where t is in days, k_2 and q are the apsidal coefficient and the mass ratio, respectively. Compared to Eq. (4), $\text{(O–C)}_{\text{orbital}}$ should be its sinusoidal part. Thus, Ω is found to be 9.74×10^{-4} d^{-1}. Horne et al. (1993) obtained the mass ratio $q = 0.62 \pm 0.05$ for DQ Herculis. The apsidal coefficient k_2 is 0.143 for a $M \simeq 0.4\ M_\odot$ star (Warner 1988). Therefore, the amplitude of $\Delta R/R$ can be calculated to be $A = 1.43(\pm0.03)\times10^{-6}$, which is similar to the result of Warner (1988). However, Marsh & Pringle (1990) found that Warner (1988) did not consider whether enough energy is available to produce such changes on the observed time scales. Therefore, we attempted to estimate the time scale of change, t_{ch}, for DQ Herculis, which can be given by the equation (Marsh & Pringle 1990)

$$t_{\text{ch}} > 2\times10^7 f\frac{\Delta R}{R}\left(\frac{M_2^2}{L_2 R_2}\right)\ \text{yr}, \quad (10)$$

where f, M_2 and L_2 are outer mass fraction, the mass and the luminosity of the red dwarf, respectively. Schneider & Greenstein (1979) estimated the spectral type of the secondary star of DQ Herculis to be M4 or later, and Young & Schneider (1981) pointed out that its spectral type should be $M3^+V$ due to the TiO band ratio found. This means that the luminosity of the red dwarf can be estimated to be 1.07×10^{32} erg s^{-1}, and the red dwarf may be a fully convective star. Thus, Eq. (10) becomes

$$t_{\text{ch}} > 3.38\times10^2 f\ \text{yr}, \quad (11)$$

with $R_2 = 0.49\ R_\odot$ (Horne et al. 1993). If the observed period change is caused by a change in the mean radius of the red dwarf, then the ~17.7(±0.3) yr quasi-periodic oscillation shown in Fig. 5 indicates $f \sim 0.052$, which means that the radius change only involves an extremely thin shell (i.e. $M_{\text{shell}} \sim 0.02\ M_\odot$). This is obviously unreasonable for $a \simeq 0.4\ M_\odot$ fully convective red dwarf star. Thus, a change in the size of the red dwarf of DQ Herculis requires too much energy. This further supports the conclusions of Hall (1991) and Marsh & Pringle (1990).

4.2.2. Applegate's mechanism

Since Marsh & Pringle (1990) pointed out the required energy problem, Applegate (1992) proposed an alterative mechanism, which is magnetic activity-driven change in the quadrupole momentum of the red dwarf. According to this mechanism, the relationship between the orbital period P and the variation of the quadrupole momentum ΔQ is given by

$$\frac{\Delta P}{P} = -9\left(\frac{R_2}{a}\right)^2\frac{\Delta Q}{M_2 {R_2}^2}, \quad (12)$$

where R_2 and a are the radius of the secondary star and the binary separation, respectively. Using $a = 1.41(\pm0.05)\ R_\odot$ and $M_2 = 0.40(\pm0.05)\ M_\odot$ (Horne et al. 1993), ΔQ can be calculated to be $-7.4(\pm1.1)\times10^{40}$ g cm^2.

In order to discuss the internal angular momentum transport, which can produce the orbital period variation in a fully convective star, the whole star is split into an inner core and an outer shell. The energy ΔE required to cause the angular momentum transfer ΔJ between the shell and core, is estimated by the formula (Applegate 1992)

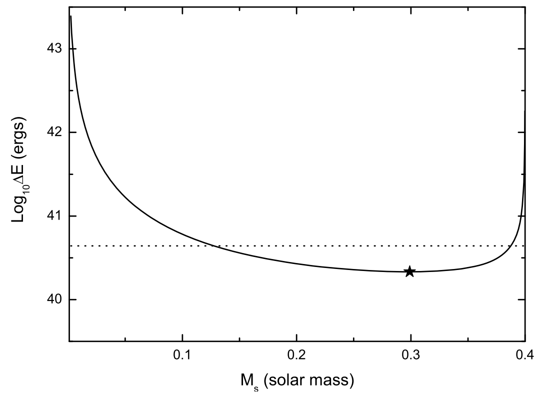

Fig. 6. The correlation between the energy required to produce the orbital period oscillation of DQ Herculis by using the Applegate (1992) mechanism and the assumed different shell masses of the fully convective red dwarf (solid line). The star denotes the minimum required energy, and the dotted line is the total radiant energy of the red dwarf over the whole oscillation period.

$$\Delta E = \Omega_{\text{dr}}\Delta J + \frac{(\Delta J)^2}{2I_{\text{eff}}}, \quad (13)$$

where $\Omega_{\text{dr}} = \Omega_{\text{shell}} - \Omega_{\text{core}}$ is the initial differential rotation, and $I_{\text{eff}} = I_{\text{shell}}I_{\text{core}}/(I_{\text{shell}}+I_{\text{core}})$ is the reduced rotational inertia. The required energy ΔE versus each different shell mass M_s is plotted in Fig. 6. The lowest required energy $\Delta E_{\min}$ is 2.15×10^{40} erg at $M_s \simeq 0.30\ M_\odot$. Assuming that the spectral type of the red dwarf is M3V, the total radiant energy E_0 in a complete variation period of 17.7 yr, which is the maximum energy offered by the luminosity variations of the M3V-type red dwarf, can be estimated to be 5.95×10^{40} erg. The apparent magnitude variation of DQ Herculis is $\Delta m_v \simeq 0.6$ (Warner 1988), which gives the energy emitted by the red dwarf of $E_0 \simeq 4.39\times10^{40}$ erg. Since E_0 of is the same order of magnitude as $\Delta E_{\min}$, we consider that Applegate's mechanism may have difficulty in explaining the observed oscillation in orbital period (i.e. $E_0/\Delta E_{\min} \sim 2$).

4.2.3. Light travel-time effect

Another plausible mechanism to explain the sinusoidal variation in the O–C diagram is the light travel-time effect, which is caused by a perturbations from a tertiary component (Irwin 1952; Borkovits & Hegedues 1996). Patterson et al. (1978) suggested that the light travel-time effect is not a good explanation for the periodic oscillation in the O–C diagram of DQ Herculis because no evidence for a similar sinusoidal variation is found in the O–C diagram of 71 s. However, the detection of 71 s has a large error because of the very short time scale and the large oscillation phase shifts, which may affect the continuity of the times of maximum and the precision of the ephemeris. Moreover, there is no clear evidence that the O–C diagrams of 71 s well reflect the motion of the mass-center of DQ Herculis. Therefore, we investigated the possible light travel-time effect.

The strictly sinusoidal fit presented in Fig. 5 is a special case that corresponds to the assumption of a circular orbit. We assumed that the small departure near 60 000 cycles shown in the top panel of Fig. 5 is caused by a small orbital eccentricity of the third body, which can be described by (Irwin 1952);

$$\text{O–C} = \frac{a\,\sin i}{c}\left[\frac{1-e^2}{1+e\cos\nu}\sin(\nu+\omega) + e\,\sin\omega\right], \quad (14)$$

Table 2. The best-fit coefficients.

	Coefficients	Errors
a_0	0.00201	0.00002
α	-9.6×10^{-8}	0.1×10^{-8}
β	9.3×10^{-13}	0.1×10^{-13}
a_1	−0.00084	0.00002
b_1	−0.00037	0.00001
a_2	−0.00003	0.00001
b_2	−0.00004	0.00001

where a, c, i, e, ν and ω are the semi-major axis of elliptic orbit, light speed, orbital inclination, eccentricity, true anomaly and the longitude of periastron from the ascending node. If the assumed orbital eccentricity is small enough (i.e. $e < 0.6$), then Eq. (9) can be replaced with a simple approximate formula (Kopal 1959, 1978),

$$\mathrm{O{-}C} = a_0 + a_1\cos(\Omega\, E) + b_1\sin(\Omega\, E) + a_2\cos(2\Omega\, E) + b_2\sin(2\Omega\, E), \tag{15}$$

where Ω is the angular frequency of elliptic orbit, which corresponds to the orbital period of the third body, P_3. $a\sin i$ is the projected distance from the binary pair to the mass-center of this triple system. $a\sin i$, e and ω can be given by

$$a\sin i = c\sqrt{a_1^2 + b_1^2}, \tag{16}$$

$$e = 2\sqrt{\frac{a_2^2 + b_2^2}{a_1^2 + b_1^2}}, \tag{17}$$

$$\omega = \arctan\left(\frac{b_2(b_1^2 - a_1^2) + 2a_1a_2b_1}{a_2(a_1^2 - b_1^2) + 2a_1b_1b_2}\right). \tag{18}$$

Based on the above O–C analysis, a quadratic term should be added to Eq. (15), which leads to:

$$\mathrm{O{-}C} = a_0 + \alpha\, E + \beta\, E^2 + a_1\cos(\Omega\, E) + b_1\sin(\Omega\, E) + a_2\cos(2\Omega\, E) + b_2\sin(2\Omega\, E), \tag{19}$$

where α and β are the coefficients of linear and quadratic terms, respectively. All best-fit coefficients are listed in Table 2. We obtained $F(6, 218) = 16.2$, which corresponds to $a \sim 99.99\%$ confidence level for a quadric-plus-eccentric fit. The mass function of the third component, $f(m_3)$, can be estimated by the formula

$$f(m_3) = \frac{4\pi^2}{GP_3^2} \times (a\sin(i))^3. \tag{20}$$

Since the eccentricity $e = 0.12$ is near zero, the elliptic orbit should be close to the circular orbit. Accordingly, the parameters of the third body derived from an eccentric fit are similar to that derived from a strictly sinusoidal fit (see Table 3). In addition, the χ^2 values for the eccentric fit and strictly sinusoidal fit are nearly the same. This means that the elliptic orbit of the third body with eccentricity $e = 0.12$ also cannot explain the departure near 60 000 cycles in the O–C diagram. Therefore, this episode may imply a sudden change in the orbital period of DQ Herculis caused by an unknown mechanism. Assuming a combined mass of $0.6(\pm 0.07)\ M_\odot + 0.4(\pm 0.05)\ M_\odot$ for the eclipsing pair of DQ Herculis (Horne et al. 1993), the relationship between the mass of the third body, M_3, and its orbital inclination, i, is displayed in the left panel of Fig. 7. The third body in DQ Herculis could be a brown dwarf, as long as $i > 20°$, which implies that it is a brown dwarf with a confidence level $\gtrsim 77.8\%$ based on the inclination, and its distance from the binary system shown in the right panel of Fig. 7 is $\sim 6.49(\pm 0.95)$ au, nearly 10^3 times the binary separation. Since the red dwarf of DQ Herculis should be a low mass main sequence star, it cannot expand too much to swallow the remote third body when it reaches the red giant stage. This indicates that the brown dwarf could have survived the common envelope evolution of the parent binary. Assuming an orbit of the third body almost coplanar to the nova DQ Herculis with inclination $i \approx 86.5°$ (Horne et al. 1993), the third body may be a massive extrasolar planet with a mass of $M_3 \simeq 0.02\ M_\odot$, which is ~20 times larger than that of Jupiter.

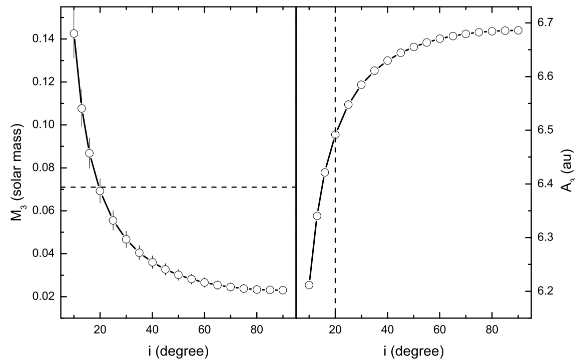

Fig. 7. The relationship between the mass of the third body and its orbital inclination in the left panel, and the distances between the third body and mass center corresponding to different inclinations are in the right panel. The dashed line in the left and right panels denotes the upper limit of the masses of the brown dwarf (~0.071 $M_\odot$), and $i = 20°$, respectively.

Table 3. The parameters of the elliptic and circular orbit

Parameters	Circular orbit	Elliptical orbit
ω		−1.4(3)
e	0	0.12(6)
P_3 (yr)	17.7(3)	17.9(3)
$a\sin i$ (A.U.)	0.154(3)	0.159(3)
$f(m_3)$ ($M_\odot$)	0.0000116(8)	0.0000125(8)
σ	$1\overset{\mathrm{d}}{.}17 \times 10^{-3}$	$1\overset{\mathrm{d}}{.}18 \times 10^{-3}$
χ^2	36.4	36.8

5. Conclusion

All 226 available times of light minimum covering 54 years are compiled and a new O–C diagram of DQ Herculis is obtained. The fit shown in Fig. 5 implies that the best-fit of the O–C diagram is a sinusoidal variation with an ~17.7(±0.3) yr period superimposed on the secular orbital period increase. This resolves the long-term debate of whether the orbital period of DQ Herculis is increasing or not. The increased orbital period is calculated to be $9.5(\pm 0.1) \times 10^{-12}\ \mathrm{s\,s^{-1}}$. Using the absolute parameters of DQ Herculis derived by Horne et al. (1993), we estimated the lower limit of the mass transfer rate to be $7.2(\pm 3.2) \times 10^{-9}\ M_\odot\ \mathrm{yr^{-1}}$. In order to check the results of the orbital period increase presented in this paper, photometric observations with a longer base line are needed.

Although there is a small departure near 60 000 cycles, the overall trend in the O–C diagram can be well described by a quadric-plus-sinusoidal formula. Since there is no detailed analysis for the episodes of quasi-period oscillation, we investigated three plausible mechanisms, which are a red dwarf radius variation, Applegate's mechanism and the light travel-time effect, to explain the observed orbital period variation. According to the first mechanism, we concluded that the red dwarf's radius variation with an amplitude $A \sim 1.43(\pm 0.03) \times 10^{-6}$ is sufficient to account for the small quasi-sinusoidal oscillation seen in Fig. 5. But this requires too much energy, and the time scale $t_{\rm ch}$ is far longer than the oscillation period. Thus a direct change in radius of the tidally distorted secondary star cannot explain the observed quasi-periodic variation. Then Applegate's mechanism was used to probe whether the solar-type magnetic activity is responsible for the observed modulations in the O–C diagram. However, this still gives a negative result. In order to show that the magnetic activity cycle of the red dwarf star in DQ Herculis is strong enough to cause the observed modulation in the O–C diagram, A detailed analysis of variation in its brightness is necessary. Finally, an eccentric orbit of the tertiary component with a small eccentricity was attempted to explain the small departure displayed in the top panel of Fig. 5. The derived orbital eccentricity, $e = 0.12$, is small enough, which means that the parameters of the third body derived from an elliptic orbit are similar to that derived from the circular orbit (see Table 3). This suggests that further studies are needed to explain the departure occurring in ~1985. Based on the analysis of the light travel-time effect, a brown dwarf as a third component of the system is possible, with a significance level of $\gtrsim 77.8\%$. Alternatively, the third body may be a massive extrasolar planet, as long as the orbital inclination of the third body is high enough. However, more convincing evidence, for example, further studies on the behavior of the 71 s oscillation in DQ Herculis, are needed to confirm the results in this paper.

Acknowledgements. This work was partly Supported by Special Foundation of the President of the Chinese Academy of Sciences and West Light Foundation of The Chinese Academy of Sciences, Yunnan Natural Science Foundation (2008CD157), the Yunnan Natural Science Foundation (No. 2005A0059M) and Chinese Natural Science Foundation (No.10573032, No. 10573013 and No.10433030). CCD photometric observations of DQ Herculis were obtained with the 1.0-m telescope at Yunnan Observatory.We thank the referee very much for the helpful comments and suggestions that helped to improve this paper greatly.

References

Africano, J., & Olson, E. 1981, PASP, 93, 130
Applegate, J. H. 1992, ApJ, 385, 621
Bianchini, A., Mastrantonio, E., Canterna, R., Stute, J., & Cantrell, K. 2004, A&A, 426, 669
Borkovits, T., & Hegedues, T. 1996, A&AS, 120, 63
Campbell, L. 1935, Harvard College Observatory Bulletin, 898, 20
Dibai, É. A., & Shakhovskoi, N. M. 1966, SvA, 10, 1059
Diethelm, R. 2003, IBVS, 5438
Diethelm, R. 2004, IBVS, 5543
Hall, D. S. 1991, ApJ, 380, L85
Horne, K., Welsh, W. F., & Wade, R. A. 1993, ApJ, 410, 357
Irwin, J. B. 1952, ApJ, 116, 211
Kopal, Z. 1959, Close Binary Systems (London: Chapman & Hall).
Kopal, Z. 1978, Dynamics of Close Binary Systems, D. Reidel. Co.
Kraft, R. P. 1959, ApJ, 130, 110
Livio, M. 1992, in Interacting Binaries, 22nd SF Advanced Course, ed. H. Nussbaumer
Locher, K. 1978, BBSAG Bull., 39, 4
Locher, K. 1979, BBSAG Bull., 42, 2
Locher, K. 1979, BBSAG Bull., 43, 2
Locher, K. 1979, BBSAG Bull., 44, 3
Locher, K. 1979, BBSAG Bull., 45, 4
Locher, K. 1980, BBSAG Bull., 46, 3
Locher, K. 1980, BBSAG Bull., 47, 3
Locher, K. 1980, BBSAG Bull., 48, 2
Locher, K. 1980, BBSAG Bull., 49, 4
Locher, K. 1980, BBSAG Bull., 50, 3
Locher, K. 1981, BBSAG Bull., 54, 2
Locher, K. 1981, BBSAG Bull., 55, 2
Locher, K. 1981, BBSAG Bull., 56, 5
Locher, K. 1981, BBSAG Bull., 57, 4
Locher, K. 1982, BBSAG Bull., 58, 3
Locher, K. 1982, BBSAG Bull., 59, 2
Locher, K. 1982, BBSAG Bull., 60, 3
Locher, K. 1982, BBSAG Bull., 61, 3
Locher, K. 1982, BBSAG Bull., 63, 2
Locher, K. 1983, BBSAG Bull., 64, 4
Locher, K. 1983, BBSAG Bull., 65, 3
Locher, K. 1983, BBSAG Bull., 66, 3
Locher, K. 1983, BBSAG Bull., 67, 3
Locher, K. 1983, BBSAG Bull., 68, 4
Locher, K. 1983, BBSAG Bull., 69, 4
Locher, K. 1984, BBSAG Bull., 71, 2
Locher, K. 1984, BBSAG Bull., 72, 2
Locher, K. 1984, BBSAG Bull., 73, 4
Locher, K. 1984, BBSAG Bull., 84, 3
Locher, K. 1985, BBSAG Bull., 77, 4
Locher, K. 1986, BBSAG Bull., 80, 3
Locher, K. 1986, BBSAG Bull., 81, 3
Locher, K. 1986, BBSAG Bull., 82, 4
Locher, K. 1987, BBSAG Bull., 83, 3
Locher, K. 1987, BBSAG Bull., 84, 3
Locher, K. 1987, BBSAG Bull., 85, 3
Locher, K. 1988, BBSAG Bull., 88, 4
Locher, K. 1988, BBSAG Bull., 89, 7
Locher, K. 1989, BBSAG Bull., 92, 3
Locher, K. 1990, BBSAG Bull., 94, 3
Locher, K. 1990, BBSAG Bull., 95, 3
Locher, K. 1990, BBSAG Bull., 96, 5
Locher, K. 1991, BBSAG Bull., 97, 6
Locher, K. 1991, BBSAG Bull., 98, 7
Locher, K. 1993, BBSAG Bull., 104, 5
Locher, K. 1994, BBSAG Bull., 106, 5
Locher, K. 1994, BBSAG Bull., 107, 8
Locher, K. 1995, BBSAG Bull., 108, 7
Locher, K. 1995, BBSAG Bull., 109, 9
Locher, K. 1996, BBSAG Bull., 112, 7
Locher, K. 1997, BBSAG Bull., 114, 8
Locher, K. 1998, BBSAG Bull., 117, 8
Locher, K. 1998, BBSAG Bull., 118, 6
Locher, K. 2000, BBSAG Bull., 121, 6
Locher, K. 2001, BBSAG Bull., 126, 5
Locher, K. 2002, BBSAG Bull., 127, 5
Marsh, T. R., & Pringle, J. E. 1990, ApJ, 365, 677
Martin, P. G. 1989, in Classical Novae, ed. M. F. Bode, & A. Evans (Chichester: Wiley), Chap. 6
Mumford, G. S. 1969, in Mass Loss from Stars, ed. M. Hack (Dordrecht: Reidel Publishing Co.), 204
Nagai, K. 2006, Var. Star. Bull. Japan, 44
Nather, R. E., & Warner, B. 1969, MNRAS, 143, 145
Nelson, M. R., & Olson, E. C. 1976, ApJ, 207, 195
Patterson, J. 1994, PASP, 106, 209
Patterson, J., Robinson, E. L., & Nather, R. E. 1978, ApJ, 224, 570
Pringle, J. E. 1975, MNRAS, 170, 633
Robinson, E. L. 1976, ApJ, 203, 485
Schneider, D. P., & Greenstein, J. L. 1979, ApJ, 233, 935
Schoembs, R., & Rebhan, H. 1989, A&A, 224, 42
Smak, J. 1971, Acta Astron., 21, 15
Smak, J. 1980, Acta Astron., 30, 267
Smak, J. 2004, Acta Astron., 54, 433
Starrfield, S, 1989, in Classical Novae, ed. M. F. Bode, & A. Evans (Chichester: Wiley), Chap. 3
Swedlund, J. B., Kemp, J. C., & Wolstencroft, R. D. 1974, ApJ, 193, 11
Vaytet, N. M. H., O'Brien, T. J., & Rushton, A. P. 2007, MNRAS, 380, 175
Walker, M. F. 1956, ApJ, 123, 68
Walker, M. F. 1958, ApJ, 127, 319
Warner, B. 1988, Nature 336, 10
Warner, B., & Nather, R. E. 1971, MNRAS, 152, 219
Warner, B., Peters, W. L., Hubbard, W. B, & Nather, R. E. 1972, MNRAS, 159, 321
Wood, M. A., Robertson, J. R., & Simpson, J. C., et al. 2005, ApJ, 634, 570
Young, P. J., Schneider, D. P. 1981, ApJ, 247, 960
Zhang, E., Robinson, E. L., Stiening, R. F., & Horne, K. 1995, ApJ, 454, 447

Table 1. The times of light minimum for the old nova DQ Herculis.

JD. Hel. 2 400 000+	Type	Error	method	E (cycle)	(O–C)^d	Ref.	JD. Hel. 2 400 000+	Type	Error	Method	E (cycle)	(O–C)^d	Ref.
34954.751500	pri		pe	−1	0.00204	(1)	42189.974640	pri		pe	37367	−0.00139	(6)
34954.944950	pri		pe	0	0.00184	(1)	42191.910790	pri		pe	37377	−0.00150	(6)
34955.719060	pri		pe			(2)	42193.072620	pri		pe	37383	−0.00140	(6)
34955.719100	pri		pe			(3)	42223.665520	pri	0.00068	pe	37541	−0.00057	(3)
34955.718940^{cr}	pri		pe	4	0.00139	(1)	42245.737350	pri		pe	37655	−0.00150	(3)
34981.665000	pri		pg	138	0.00223	(1)	42329.576020	pri		pe	38088	−0.00071	(3)
34983.794960	pri		pe	149	0.00233	(1)	42342.548590	pri		pe	38155	−0.00075	(3)
34984.762980	pri		pe	154	0.00233	(1)	42513.903900	pri		pe	39040	0.00004	(3)
34985.729820	pri		pe	159	0.00103	(1)	42514.872200	pri		pe	39045	0.00024	(3)
34989.797000	pri		pg	180	0.00213	(1)	42515.840500	pri		pe	39050	0.00043	(3)
35218.851030	pri		pe	1363	0.00260	(2)	42569.858820	pri		pe	39329	−0.00144	(3)
35243.827480	pri		pe	1492	0.00200	(2)	42571.794290	pri		pe	39339	−0.00224	(3)
35374.715180	pri		pe	2168	0.00198	(2)	42593.675500	pri		pe	39452	−0.00017	(3)
35659.917250	pri		pe	3641	0.00040	(2)	42605.679900	pri		pe	39514	−0.00027	(3)
35660.691900	pri		pe	3645	0.00057	(2)	42606.841700	pri		pe	39520	−0.00020	(3)
35660.884980	pri		pe	3646	0.00003	(2)	42662.602780	pri		pe	39808	−0.00196	(3)
35695.736950	pri		pe	3826	0.00024	(2)	42925.928210	pri		pe	41168	−0.00097	(3)
35695.930620	pri		pe	3827	0.00029	(2)	42926.896650	pri		pe	41173	−0.00063	(3)
35696.705600	pri		pe	3831	0.00078	(2)	42927.865260	pri		pe	41178	−0.00013	(3)
35697.673600	pri		pe	3836	0.00068	(2)	42928.833320	pri		pe	41183	−0.00017	(3)
35697.867250	pri		pe	3837	0.00071	(2)	42929.801430	pri		pe	41188	−0.00017	(3)
36103.696500	pri		pe	5933	0.00051	(3)	42934.835800	pri		pe	41214	0.00006	(3)
36351.918500	pri		pe	7215	0.00048	(3)	42935.803800	pri		pe	41219	−0.00004	(3)
36376.894800	pri		pe	7344	−0.00032	(3)	42955.747400	pri		pe	41322	0.00060	(3)
36393.740200	pri		pe	7431	0.00006	(3)	42991.760200	pri		pe	41508	−0.00009	(3)
36399.742400	pri		pe	7462	0.00002	(3)	42993.696900	pri		pe	41518	0.00040	(3)
36407.874300	pri		pe	7504	−0.00016	(3)	42994.665000	pri		pe	41523	0.00039	(3)
36487.646200	pri		pe	7916	−0.00008	(3)	43007.637100	pri		pe	41590	−0.00011	(3)
36785.822800	pri		pe	9456	0.00030	(3)	43310.847760	pri		pe	43156	0.00019	(3)
39060.288600	pri		pe	21203	0.00113	(4)	43716.870520	pri	0.00015	pe	45253	−0.00012	(3)
40006.900700	pri		pe	26092	0.00055	(3)	43808.261000	pri		pv	45725	0.00130	(7)
40007.868600	pri		pe	26097	0.00034	(3)	43913.008800	pri		pe	46266	0.00016	(3)
40070.795600	pri		pe	26422	0.00054	(3)	43940.505000	pri		pv	46408	0.00218	(8)
40073.699700	pri		pe	26437	0.00033	(3)	43942.634000	pri		pv	46419	0.00138	(8)
40073.892800	pri		pe	26438	−0.00019	(3)	44024.531000	pri		pe	46842	−0.00333	(9)
40074.668100	pri		pe	26442	0.00062	(3)	44054.739600	pri		pe	46998	0.00045	(3)
40074.861700	pri		pe	26443	0.00060	(3)	44073.525000	pri		pv	47095	0.00466	(10)
40417.763000	pri		pe	28214	−0.00076	(3)	44079.525000	pri		pv	47126	0.00236	(10)
40418.925500	pri		pe	28220	0.00002	(3)	44082.429000	pri		pv	47141	0.00206	(10)
40441.772000	pri		pe	28338	−0.00075	(3)	44100.819670	pri		pe	47236	−0.00126	(3)
40443.901500	pri		pe	28349	−0.00107	(3)	44105.662400	pri		pe	47261	0.00096	(3)
40444.676500	pri		pe	28353	−0.00056	(3)	44110.695800	pri		pe	47287	0.00020	(3)
40444.870500	pri		pe	28354	−0.00018	(3)	44111.665000	pri		pe	47292	0.00126	(3)
40445.645000	pri		pe	28358	−0.00017	(3)	44111.857400	pri		pe	47293	0.00008	(3)
40445.838500	pri		pe	28359	−0.00029	(5)	44139.738200	pri		pe	47437	−0.00054	(3)
40446.806000	pri		pe	28364	−0.00089	(3)	44140.706900	pri		pe	47442	0.00005	(3)
41215.675000	pri		pe	32335	−0.00057	(3)	44142.643800	pri		pe	47452	0.00075	(3)
41220.709000	pri		pe	32361	−0.00072	(3)	44143.420000	pri		pv	47456	0.00245	(11)
41917.743940	pri		pe	35961	−0.00110	(3)	44267.723000	pri		pv	48098	0.00084	(12)
41918.712160	pri		pe	35966	−0.00098	(3)	44289.602000	pri		pv	48211	0.00064	(12)
41945.625760	pri		pe	36105	−0.00069	(3)	44341.493000	pri		pv	48479	0.00123	(13)
41948.723150	pri		pe	36121	−0.00126	(3)	44343.428000	pri		pv	48489	0.00006	(13)
41979.703400	pri		pe	36281	−0.00033	(3)	44370.537000	pri		pv	48629	0.00212	(14)
41980.671000	pri		pe	36286	−0.00084	(3)	44396.482000	pri		pv	48763	0.00192	(14)
41981.639400	pri		pe	36291	−0.00054	(3)	44456.507000	pri		pv	49073	0.00441	(15)
42130.144420	pri		pe	37058	−0.00279	(6)	44461.538000	pri		pv	49099	0.00131	(15)
42131.112510	pri		pe	37063	−0.00279	(6)	44466.573000	pri		pv	49125	0.00211	(15)
42132.080600	pri		pe	37068	−0.00279	(6)	44487.483000	pri		pv	49233	0.00111	(16)
42161.124630	pri		pe	37218	−0.00189	(6)	44704.532000	pri		pv	50354	0.00108	(17)
42162.092710	pri		pe	37223	−0.00189	(6)	44770.556000	pri		pv	50695	0.00030	(18)
42163.060790	pri		pe	37228	−0.00199	(6)	44809.474500	pri		pv	50896	0.00097	(19)
42164.028880	pri		pe	37233	−0.00199	(6)	44812.572000	pri		pv	50912	0.00057	(19)
42164.996960	pri		pe	37238	−0.00199	(6)	44819.542000	pri		pv	50948	0.00021	(19)
44848.392000	pri		pv	51097	0.00066	(19)	46649.452000	pri		pv	60399	−0.00113	(40)
44853.428000	pri		pv			(19)	46651.580000	pri		pv	60410	−0.00297	(41)
44853.429000	pri		pv			(19)	46907.549000	pri		pv	61732	−0.00082	(42)
44853.428500^{cr}	pri		pv	51123	0.00306	(19)	46952.469000	pri		pv	61964	−0.00087	(43)
44885.374000	pri		pv	51288	0.00106	(20)	47037.468000	pri		pv	62403	−0.00146	(44)

Table 1. continued.

JD. Hel. 2 400 000+	Type	Error	Method	E (cycle)	(O–C)^d	Ref.	JD. Hel. 2 400 000+	Type	Error	Method	E (cycle)	(O–C)^d	Ref.
– 44895.249000	pri		pv	51339	0.00146	(21)	47304.472000	pri		pv	63782	−0.00070	(45)
44910.351000	pri		pv	51417	0.00096	(20)	47383.467000	pri		pv	64190	−0.00306	(46)
45053.631000	pri		pv	52157	0.00154	(22)	47746.507000	pri		pv	66065	−0.00231	(47)
45101.456000	pri		pv	52404	0.00213	(23,24)	47942.643000	pri		pv	67078	−0.00423	(48)
45140.373000	pri		pv	52605	0.00133	(24)	48039.457000	pri		pv	67578	−0.00073	(49)
45142.890400[+]	pri		pe	52618	0.00163	(25)	48123.488000	pri		pv	68012	−0.00121	(50)
45144.826400[+]	pri		pe	52628	0.00143	(25)	48306.653000	pri	0.001	pv	68958	−0.00160	(51)
45203.686700[+]	pri		pe	52932	0.00102	(25)	48384.875600[+]	pri		pe	69362	−0.00185	(25)
45233.697600[+]	pri		pe	53087	0.00061	(25)	48385.844000[+]	pri		pe	69367	−0.00155	(25)
45234.666000[+]	pri		pe	53092	0.00091	(25)	48390.492000	pri	0.001	pv	69391	−0.00045	(52)
45257.321000	pri		pv	53209	0.00231	(26)	48776.765600[+]	pri		pe	71386	−0.00059	(25)
45356.647000	pri		pv	53722	0.00080	(27)	49158.393000	pri	0.001	pv	73357	0.00001	(53)
45404.470000	pri		pv	53969	−0.00060	(28)	49475.546000	pri	0.003	pv	74995	0.00187	(54)
45404.666000	pri		pv			(28)	49476.898900[+]	pri		pe	75002	−0.00055	(25)
45404.667000	pri		pv			(28)	49477.866400[+]	pri		pe	75007	−0.00115	(25)
45404.666500[cr]	pri		pv	53970	0.00229	(28)	49568.481000	pri	0.002	pv	75475	−0.00114	(55)
45459.460000	pri		pv	54253	0.00108	(29)	49799.474000	pri	0.002	pv	76668	0.00213	(56)
45499.732200[+]	pri		pe	54461	0.00011	(25)	49836.453000	pri	0.002	pv	76859	−0.00050	(57)
45499.925600[+]	pri		pe	54462	−0.00011	(25)	50278.489000	pri	0.001	pe	79142	−0.00106	(58)
45500.700400[+]	pri		pe	54466	0.00020	(25)	50539.491000	pri	0.001	pv	80490	−0.00007	(59)
45500.893200[+]	pri		pe	54467	−0.00062	(25)	50630.686760[+]	pri		pe	80961	0.00022	(60)
45501.862200[+]	pri		pe	54472	0.00028	(25)	50630.881350[+]	pri		pe	80962	0.00122	(60)
45502.829900[+]	pri		pe	54477	−0.00013	(25)	50631.655040[+]	pri		pe	80966	0.00042	(60)
45503.798000[+]	pri		pe	54482	−0.00013	(25)	50631.848880[+]	pri		pe	80967	0.00062	(60)
45506.896000[+]	pri		pe	54498	-0.00006	(25)	50632.430600	pri	0.0003	pe	80970	0.00152	(61)
45547.557000	pri		pv	54708	0.00057	(30)	50633.397620[+]	pri		pe	80975	0.00042	(60)
45548.330500	pri		pv	54712	−0.00045	(31)	50633.785110[+]	pri		pe	80977	0.00062	(60)
45564.403000	pri		pv	54795	0.00147	(31)	50634.172100[+]	pri		pe	80979	0.00042	(60)
45610.290000	pri		pv	55032	0.00037	(32)	50634.753100[+]	pri		pe	80982	0.00052	(60)
45621.326000	pri		pv			(32)	50635.140380[+]	pri		pe	80984	0.00062	(60)
45621.327000	pri		pv			(32)	50636.302000[+]	pri		pe	80990	0.00052	(60)
45621.326500[cr]	pri		pv	55089	0.00046	(32)	50636.495800[+]	pri		pe	80991	0.00062	(60)
45701.674000	pri		pv	55504	-0.00475	(33)	50637.270320[+]	pri		pe			(60)
45753.569000	pri		pv	55772	−0.00012	(34)	50637.270380[+]	pri		pe			(60)
45766.538000	pri		pv			(34)	50637.270350[cr]	pri		pe	80995	0.00072	(60)
45766.540000	pri		pv			(34)	50637.463720[+]	pri		pe	80996	0.00042	(60)
45766.541000	pri		pv			(34)	50638.238300[+]	pri		pe	81000	0.00052	(60)
45766.541000	pri		pv			(34)	50639.206300[+]	pri		pe	81005	0.00042	(60)
45766.543000	pri		pv			(34)	50925.570000	pri	0.002	pv	82484	−0.00119	(62)
45766.543000	pri		pv			(34)	50954.421000	pri	0.002	pv	82633	0.00028	(63)
45766.541000[cr]	pri		pv	55839	−0.00072	(34)	51458.416000	pri	0.001	pv	85236	0.00001	(64)
45868.387000	pri		pv	56365	0.00063	(35)	52202.309000	pri	0.001	pv	89078	0.00142	(65)
45905.560000	pri		pv	56557	−0.00154	(36)	52348.491000	pri	0.002	pv	89833	−0.00030	(66)
45906.528000	pri		pv	56562	−0.00165	(36)	52413.548200	pri	0.0005	pe	90169	0.00019	(67)
46256.400000	pri		pv	58369	−0.00262	(37)	52763.421000	pri	0.001	pv	91976	0.00005	(68)
46590.397000	pri		pv	60094	−0.00174	(38)	52809.698340[+]	pri		pe	92215	0.00194	(60)
46622.344000	pri		pv			(38)	52809.892000[+]	pri		pe	92216	0.00204	(60)
46622.345000	pri		pv			(38)	52810.666560[+]	pri		pe	92220	0.00204	(60)
46622.344500[cr]	pri		pv	60259	−0.00169	(38)	52810.860280[+]	pri		pe	92221	0.00214	(60)
46626.603700[+]	pri	0.0005	pe			(25)	52815.700700[+]	pri		pe	92246	0.00204	(60)
46626.603100	pri	0.0005	pe	60281	−0.00277	(39)	52815.894410[+]	pri		pe	92247	0.00214	(60)
46627.571400[+]	pri	0.0004	pe			(25)	53149.502000	pri	0.001	pv	93970	0.00090	(69)
46627.570800	pri	0.0004	pe	60286	−0.00317	(39)	53475.173100	pri		ccd	95652	0.00165	(70)
46648.483000	pri		pv			(40)	54507.364570[N]	pri	0.0001	ccd	100983	−0.00008	(71)
46648.485000	pri		pv			(+)	54554.415230[R]	pri	0.00015	ccd	101226	0.00072	(71)
46648.484000[cr]	pri		pv	60394	−0.00102	(40)							

Note. [+] HJED data. [cr] the corrected data used in this paper, which corresponds to the above data without cycles and O–C. [N] no filter used in observation. [R] the R-filter used in observation. References: (1) Swedlund et al. (1974); (2) Vaytet et al. (2007); (3) Africano & Olson (1981); (4) Dibai & Shakhovskoi (1966); (5) Walker (1958); (6) Smak (2004); (7) BBSAG Bull. 39 (1978); (8) BBSAG Bull. 42 (1979); (9) BBSAG Bull. 43 (1978); (10) BBSAG Bull. 44 (1978); (11) BBSAG Bull. 45 (1979); (12) BBSAG Bull. 46 (1980); (13) BBSAG Bull. 47 (1980); (14) BBSAG Bull. 48 (1980); (15) BBSAG Bull. 49 (1980); (16) BBSAG Bull. 50 (1980); (17) BBSAG Bull. 54 (1981); (18) BBSAG Bull. 55 (1981); (19) BBSAG Bull. 56 (1981); (20) BBSAG Bull. 57 (1981); (21) BBSAG Bull. 58 (1982); (22) BBSAG Bull. 59 (1982); (23) BBSAG Bull. 60 (1982); (24) BBSAG Bull. 61 (1982); (25) Warner (1988); (26) BBSAG Bull. 63 (1982); (27) BBSAG Bull. 64 (1983); (28) BBSAG Bull. 65 (1983); (29) BBSAG Bull. 66 (1983); (30) BBSAG Bull. 67 (1983); (31) BBSAG Bull. 68 (1983); (32) BBSAG Bull. 69 (1983); (33) BBSAG Bull. 70 (1984); (34) BBSAG Bull. 71 (1984); (35) BBSAG Bull. 72 (1984); (36) BBSAG Bull. 73 (1984); (37) BBSAG Bull. 77 (1985); (38) BBSAG Bull. 80 (1986); (39) Robinson (1976); (40) BBSAG Bull. 82 (1986); (41) BBSAG Bull. 81 (1986); (42) BBSAG Bull. 83 (1987); (43) BBSAG Bull. 84 (1987); (44) BBSAG Bull. 85 (1987); (45) BBSAG Bull. 88 (1988); (46) BBSAG Bull. 89 (1988); (47) BBSAG Bull. 92 (1989); (48) BBSAG Bull. 94 (1990); (49) BBSAG Bull. 95 (1990); (50) BBSAG Bull. 96 (1990); (51) BBSAG Bull. 97 (1991); (52) BBSAG Bull. 98 (1991); (53) BBSAG Bull. 104 (1993); (54) BBSAG Bull. 106 (1994); (55) BBSAG Bull. 107 (1994); (56) BBSAG Bull. 108 (1995); (57) BBSAG Bull. 109 (1995); (58) BBSAG Bull. 112 (1996); (59) BBSAG Bull. 114 (1997); (60) Wood et al. (2005); (61) Krzesinski unpublished (1999); (62) BBSAG Bull. 117 (1998); (63) BBSAG Bull. 118 (1998); (64) BBSAG Bull. 121 (2000); (65) BBSAG Bull. 126 (2001); (66) BBSAG Bull. 127 (2002); (67) Bianchini et al. (2004); (68) Diethelm (2003); (69) Diethelm (2004); (70) Nagai (2006); (71) This paper.